NIH Public Access
Author Manuscript
DNA Repair (Amst). Author manuscript; available in PMC 2011 February 16.

Published in final edited form as:
DNA Repair (Amst). 2006 December 9; 5(12): 1407–1420. doi:10.1016/j.dnarep.2006.06.009.

Quantitative determination of uracil residues in *Escherichia coli* DNA: Contribution of *ung*, *dug*, and *dut* genes to uracil avoidance☆

Sibghat-Ullah Lari[a], **Cheng-Yao Chen**[a,1], **Béata G. Vertéssy**[b], **Jeff Morré**[c], and **Samuel E. Bennett**[a,c,*]

[a] Department of Environmental and Molecular Toxicology, Oregon State University, Corvallis, OR 97331-7301, United States

[b] Institute of Enzymology, Biological Research Center, Hungarian Academy of Science, Budapest, Hungary

[c] Environmental Health Sciences Center, Oregon State University, Corvallis, OR 97331-7302, United States

Abstract

The steady-state levels of uracil residues in DNA extracted from strains of *Escherichia coli* were measured and the influence of defects in the genes for uracil-DNA glycosylase (*ung*), double-strand uracil-DNA glycosylase (*dug*), and dUTP pyrophosphatase (*dut*) on uracil accumulation was determined. A sensitive method, called the Ung-ARP assay, was developed that utilized *E. coli* Ung, T4pdg, and the Aldehyde Reactive Probe reagent to label a basic sites resulting from uracil excision with biotin. The limit of detection was one uracil residue per million DNA nucleotides (U/10^6 nt). Uracil levels in the genomic DNA of *E. coli* JM105 (*ung*$^+$ *dug*$^+$) were at the limit of detection, as were those of an isogenic *dug* mutant, regardless of growth phase. Inactivation of *ung* in JM105 resulted in 31 ± 2.6 U/10^6 nt during early log growth and 19 ± 1.7 U/10^6 nt in saturated phase. An *ung dug* double mutant (CY11) accumulated 33 ± 2.9 U/10^6 nt and 23 ± 1.8 U/10^6 nt during early log and saturated phase growth, respectively. When cultures of CY11 were supplemented with 20 ng/ml of 5-fluoro-2′-deoxyuridine, uracil levels in early log phase growth DNA rose to 125 ± 1.7 U/10^6 nt. Deoxyuridine supplementation reduced the amount of uracil in CY11 DNA, but uridine did not. Levels of uracil in DNA extracted from CJ236 (*dut-1 ung-1*) were determined to be 3000–8000 U/10^6 nt as measured by the Ung-ARP assay, two-dimensional thin-layer chromatography of metabolically-labeled ^{32}P DNA, and LC/MS of uracil and thymine deoxynucleosides. DNA sequencing revealed that the sole molecular defect in the CJ236 dUTP pyrophosphatase gene was a C→T transition mutation that resulted in a Thr24Ile amino acid change.

Keywords

Uracil; Uracil-DNA glycosylase; Double-strand uracil-DNA; glycosylase; dUTP pyrophosphatase; Aldehyde Reactive Probe (ARP); Chemiluminescence

☆This work was supported by National Institute of General Medical Sciences Grant GM66245 (to S.E.B.) and Howard Hughes Medical Institutes Grant 55005628 (to B.G.V.).

*Corresponding author. Tel.: +1 541 737 1797; fax: +1 541 737 0497. bennetsa@onid.oregonstate.edu (S.E. Bennett).
[1]Present address: Department of Pathology, University of Washington, Seattle, WA 98195-7705, United States.

NIH-PA Author Manuscript
NIH-PA Author Manuscript
NIH-PA Author Manuscript

NIH-PA Author Manuscript

NIH-PA Author Manuscript

NIH-PA Author Manuscript

1. Introduction

Uracil residues are introduced into genomic DNA through incorporation of dUMP in place of dTMP by DNA polymerases during replication, and by deamination of existing dCMP residues [1,2]. In bacteria such as *Escherichia coli* and *Salmonella typhimurium*, dUTP biosynthesis is an obligatory intermediate in the *de novo* synthesis of dTTP [3–5]. Since DNA polymerases can utilize dUTP in place of dTTP [6,7], some incorporation of dUMP into the bacterial chromosome is unavoidable. Studies performed *in vivo* or with cell-free systems have shown that the frequency of dUMP incorporation depends largely on the relative sizes of the intracellular dUTP and dTTP pools [8,9]. The intracellular concentration of dUTP in *E. coli* is governed by deoxycytidine triphosphate deaminase (*dcd*), which converts dCTP directly to dUTP [10], and by dUTP pyrophosphatase (*dut*) activity, which hydrolyzes dUTP to dUMP and pyrophosphate [11,12]. Together, these reactions generate about 75% of the dUTP pool [13]. The balance of the dUTP pool is produced by the reduction of UDP to dUDP by ribonucleotide reductase, followed by conversion to dUTP by nucleoside diphosphate kinase [13].

Uracil residues incorporated into DNA exist transiently since they are subject to removal by the multi-step uracil-initiated DNA base excision repair (BER) process [2,14]. In *E. coli*, uracil-DNA BER is initiated by uracil-DNA glycosylase (Ung), which catalyzes the hydrolytic cleavage of the *N*-glycosylic bond linking the uracil base to its cognate deoxyribose phosphate [15]. Under some conditions, *E. coli* double-strand uracil-DNA glycosylase (Dug), also called Mug, appears to serve as a backup activity for uracil excision [16]. Dug/Mug has been reported to play an anti-mutator role in stationary-phase cells [17]. In extracts of *E. coli ung dug* mutant cells, uracil-initiated BER was abolished [16]. Following uracil excision, the resultant baseless site can be cleaved by a class II apurinic/apyrimidinic (AP) endonuclease to generate a terminal 3′-hydroxyl and a deoxyribose 5′-phosphate (dRP) residue [18]. The dRP residue, together with one or more nucleotides, may be removed by the 5′–3′-exonuclease activity of DNA polymerase I (Pol I) [19] or by the deoxyribophosphodiesterase (dRPase) activity of Fpg protein [20]. A DNA repair patch, characterized as short (one nucleotide) or long (>1 nucleotide) is synthesized by DNA Pol I, and NAD^+-dependent DNA ligase (Lig) catalyzes phosphodiester bond formation to seal the DNA chain [21]. *E. coli* defective in uracil-DNA BER exhibit a mutator phenotype characterized by a predisposition towards C to T base substitutions, presumably from an accumulation of unrepaired deaminated cytosine residues in DNA [22].

Mutations in the *E. coli* dUTPase gene (*dut*) were shown to cause a large increase in dUMP incorporation into the genome [3]. Subsequently, it was found that while some *dut* mutations were lethal, their lethality could be suppressed by null mutations in the *dcd* gene which, presumably, reduced the accumulation of dUTP and, hence, uracil in DNA [10]. Interestingly, *dut* insertion mutations (null mutations) were found to be lethal, regardless of compensatory mutations such as *ung* or *dcd*, suggesting that dUTP pyrophosphatase might serve a essential function apart from its nucleotidylhydrolase activity [23]. In *Saccharomyces cerevisiae*, the *DUT1* gene is also required for viability [24]. Guillet et al. [24] isolated a viable *dut*(*1-1*) allele of the *S. cerevisiae DUT1* gene with compromised activity. The phenotype of the *dut1-1* single mutant included growth delay, cell cycle abnormalities, and a high spontaneous mutation rate inferred to result from accumulation of AP-sites cause by excision of incorporated dUMP [24].

Several different methods have been reported for detecting uracil residues in DNA, including acid hydrolysis of DNA followed by gas chromatography/mass spectrometry (GC/MS) of the derivatized nucleobases [25], *in vivo* DNA labeling with [6-^{3}H]dUrd [26], ^{32}P-postlabeling of DNA 2′-deoxynucleoside 3′-monophosphates [27], and single cell gel

NIH-PA Author Manuscript

NIH-PA Author Manuscript

NIH-PA Author Manuscript

electrophoresis [28]. In some cases, uracil-DNA glycosylase was used to selectively excise the uracil base from the DNA and create a uracil-excision-mediated apyrimidinic site. In order to monitor uracil excision, HPLC-tandem mass spectrometry [29] and GC/MS [30] techniques were developed to measure the free uracil released following the reaction with Ung. An alternative approach was developed based on the detection of the uracil-excision-mediated AP-site using covalent modification with [^{14}C]methoxyamine [31]. In this method, [^{14}C]methoxyamine reacted with the aldehydic sugar moiety of the AP-site and uracil detection was inferred from the formation of acid-insoluble [^{14}C]DNA [31]. While each technique may offer particular advantages, *in vivo* and *in vitro* radioactive labeling methods reportedly lack specificity and sensitivity [25], while methods involving mass spectrometry have yielded variable results [29,32], and may be more cumbersome as they require costly, specialized equipment.

In order to assess quantitatively the contribution of the *ung*, *dug* and *dut* genes to uracil-DNA accumulation in *E. coli*, we have developed a novel method for measuring uracil residues in DNA that is based on the approach of Kow and co-workers [33] for measuring AP-sites in DNA. The method, which we call the Ung-ARP assay, utilizes the Aldehyde reactive probe (ARP) reagent [33], an alkoxy amine attached via a flexible linker to a biotin moiety, to tag freshly created 3′-α,β-unsaturated aldehydes in DNA with biotin. The DNA aldehydes are formed by T4 pyrimidine dimer DNA glycosylase/AP-lyase cleavage of AP-sites [34] resulting from Ung-mediated uracil excision. Using this method, we analyzed the uracil content of DNA isolated from four *E. coli* strains, isogenic except with respect to *ung* and *dug*, and examined the effect of growth phase, nucleoside supplementation, and 5-fluoro-2′-deoxyuridine, an inhibitor of thymidylate synthase, on uracil accumulation. In addition, levels of uracil were determined in the DNA of *E. coli* CJ236 (*dut-1 ung-1*), which is defective in uracil-DNA glycosylase activity and has reduced, temperature sensitive, dUTP pyrophosphatase activity.

2. Materials and methods

2.1. Materials

Oligodeoxynucleotide U-23-mer (5′-CCCAGTCACGUCATTGT-AAAACG-3′) was obtained from Research Genetics. IDT synthesized the *E. coli dut* gene PCR primers 5′-CGGAGATAAA-GTCTTACCGCTTGAGCG-3′ and 5′-GCTATGACCGCAAACGA-AATGTTT CG-3′, and *dut* sequencing primers 5′-GTCTTACCG-CTTGAGCGCAAAG-3′ and 5′-CGGATGCGTATGTGTTACTGACG-AC-3′. ARP, *N*′-aminoxymethylcarbonylhydrazino D-biotin, was purchased from Dojindo Molecular Technologies, resuspended in distilled water as a 20 mM stock solution and stored at 4 °C, protected from light. Methoxyamine was purchased from Sigma, stored under vacuum at room temperature, and solubilized as needed. 5-Fluoro-2′-deoxyuridine, deoxyuridine, uridine, and thymidine were purchased from Sigma–Aldrich. Streptavidin conjugated with horseradish peroxidase (lyophilized) was purchased from Pierce Chemicals, resuspended in distilled water to a concentration of 1 mg/ml, and stored at 4 °C. Casamino acids (Difco) were solubilized at 10 g/l and filtered through activated charcoal (Norit-A). M9 minimal medium (supplemented with 1 g/l casamino acids and 20 μg/ml thiamine) was prepared as described [35]. Tris minimal medium with low phosphate content [36] was prepared as described by Warner et al. [8]. [^{32}P]orthophosphoric acid, 8500 Ci/mmol, was purchased from Perkin-Elmer; [6-^{3}H]uracil was a gift from Moravek Radiochemicals.

E. coli uracil-DNA glycosylase (fraction V) was purified as previously described by Bennett et al. [37]. The *E. coli nfo* gene encoding endonuclease IV (Nfo) was cloned from *E. coli* JM105 using PCR technology, overproduced in an *ung-defective* (*ung-151::Tn10*) mutant of BL21(DE3) as an N-terminal 8-amino acid his-tagged protein, and purified to apparent

NIH-PA Author Manuscript

NIH-PA Author Manuscript

NIH-PA Author Manuscript

homogeneity by immobilized Ni^{2+} affinity chromatography (Affiland) followed by thermal denaturation and single-strand DNA agarose chromatography as described by Levin et al. [38]. T4 pyrimidine-dimer DNA glycosylase (T4pdg) was a gift from R.S. Lloyd (Oregon Health Sciences University).

2.2. Bacterial strains

E. coli JM105 (*endA1 glnV44 sbcB15 rpsL thi-1* Δ(*lac-proAB*) [*F′ traD36 proAB+ lacIq lacZΔM15*] *hsdR4*(*rK-mK+*) [39]was obtained from W. Ream (Oregon State University), and CJ236 (BW313 (*Hfr* KL16 (*PO-45*) *dut-1 ung-1 thi-1 relA1 spoT1*) + pCJ105 [40]) from T. Kunkel (National Institute of Environmental Health Sciences). BW1067 (Hfr PO45 *thi-1 relA1 spoT1 ung-153::kan*) and BW504 (Hfr PO45 *thi-1 relA1 spoT1 ung-151::Tn10*) were gifts from B. Weiss (Emory University); BH157 (*dcm-6 thr-1 hisG4 leuB6 rpsL ara-14 supE44 lacY1 tonA31 tsx-78 galK2 galE2 xyl-5 thi-1 mtl-1 mug::mini-Tn10*) [41] was a gift from A. Bhagwat (Wayne State University). We believe that the *mug* gene is more correctly referred to as *dug*, for double-strand uracil-DNA glycosylase as this activity was originally named when first detected by Gallinari and Jiricny [42], and later characterized by Sung [43]. CY01 (*dug*) and CY10 (*ung*) were constructed from the host strain JM105 using bacteriophage P1-mediated generalized transduction [44] and the respective donor strains BH157 and BW1067. CY11 (*ung dug*) was constructed using the host strain CY01 and the donor strain BW1067.

2.3. Preparation of M13 U·A DNA

Bacteriophage M13mp2 was propagated in JM109 and M13mp2 single-stranded DNA was purified using the CTAB method as previously described [45]. Oligodeoxynucleotide U-23-mer, which contained a single uracil residue corresponding to position 80 of the *E. coli lacZα* gene, was 5′-end phosphorylated and annealed to M13mp2 single-stranded DNA to create a site-specific U·A base pair, and a primer extension reaction was conducted as previously described [46]. Cesium chloride ethidium bromide buoyant density centrifugation was performed to isolate form I and form II M13mp2 uracil-containing DNA (M13 U-DNA). Following extraction and dialysis, M13 U-DNA concentration was determined spectrophotometrically.

2.4. Isolation of bacterial DNA

Bacterial strains were propagated in M9 medium supplemented as described above and harvested at early log (OD_{600} = 0.5) or saturated growth phase (OD_{600} > 1.5), as determined by visible light (600 nm) absorbance spectrophotometry. Bacterial DNA was isolated using a PureGene reagent kit (Gentra) with one modification: the concentration of RNase A was increased 10-fold. After the PureGene procedure, DNAs were further purified by a salting out step. Briefly, a one-third volume of 6 M NaCl was added to the DNA solution, which was then subjected to high speed centrifugation. The pellet was discarded and DNA in the supernatant was ethanol precipitated, washed, and resuspended in Tris buffer (10 mM Tris–HCl, pH 7.5). DNA concentration was determined by UV-light absorbance spectrophotometry at 260 nm using the extinction coefficient 1 OD_{260} = 50 μg/ml double-stranded DNA. DNA purity was assessed by the ratio of absorbance at 260 and 280 nm, and the A_{280}/A_{260} ratio of acceptable DNA preparations ranged between 1.80 and 1.86.

2.5. Uracil-DNA standard curve construction

Pre-existing ARP-reactive sites in M13 U·A DNA and purified bacterial genomic DNA were neutralized in separate reactions (200 μl) containing Nfo (100 ng) and Pol β 8 kDa dRPase (200 ng) in buffer A (25 mM Tris–HCl (pH 7.5), 50 mM NaCl, 10 mM $MgCl_2$). After incubation at 37 °C for 30 min, freshly prepared methoxyamine was added to 10 mM, and

NIH-PA Author Manuscript

NIH-PA Author Manuscript

NIH-PA Author Manuscript

incubation was continued for another 30 min. The pre-treatment reaction was then adjusted to 300 mM sodium acetate (pH 5.2), and 2.2 volumes of ice-cold 100% ethanol were added to precipitate the DNA. After a 15 min incubation at −80 °C, the mixture was centrifuged at 18,000 × *g* for 15 min at 4 °C. The DNA pellet was washed twice with ice-cold 70% ethanol and resuspended in Tris buffer. A portion (10 μg) of each DNA preparation was then combined with *E. coli* Ung (100 ng), T4pdg (100 ng) and ARP (2 mM) in buffer A (100 μl) and reacted for 30 min at 37 °C to allow (1) Ung to excise uracil residues in the DNA, (2) the AP-lyase activity of T4pdg to cleave the Ung-mediated AP-sites, and (3) ARP to form an oxime with the 3′-α,β-unsaturated aldehyde reaction product of T4pdg. The reactions were terminated by the addition of NaCl to 300 mM and ethanol precipitation. After two 70% ethanol washes, the DNA was resuspended in Tris buffer and the DNA concentration determined by UV-light absorbance spectrophotometry (A_{260}) using triplicate sample dilutions. Control reactions containing pre-treated bacterial DNA were conducted as described above except *E. coli* Ung was omitted.

A set of uracil-DNA standards containing 0, 1, 2, 4, 8, 12, or 16 uracil residues per 10^6 nucleotides (U/10^6 nt) was prepared from purified Ung-ARP-reacted M13 U·A DNA and control bacterial DNA as follows. All standards contained 220 ng of DNA, including M13 U·A DNA and bacterial DNA, of which 100 ng aliquots were applied to the dot blot nitrocellulose membrane. To prepare the 1 U/10^6 nt standard, 1.6 ng of Ung-ARP reacted M13 U·A DNA was combined with 108.4 ng of control bacterial DNA in 220 μl of Tris buffer. The 2 U/10^6 nt standard was prepared from 3.2 ng of Ung-ARP reacted M13 U·A DNA and 106.8 ng of control bacterial DNA. The remaining uracil-DNA standards were similarly constructed by mixing the appropriate amounts of Ung-ARP reacted DNA and mock-reacted DNA. The DNA samples were then incubated at 98 °C for 5 min and subsequently placed into an ice bath. After a brief centrifugation step to collect the condensate, 220 μl of 2 M ammonium acetate was added to adjust the final concentration of ammonium acetate to 1 M. The volume of each sample was then supplemented with 440 μl of 1 M ammonium acetate, and 400 μl of the mixture was applied to dot blot membrane.

2.6. Dot blot and chemiluminescence analysis

A nitrocellulose membrane (Protran, 4 in. × 5-1/4 in.) and two sheets of gel blot filter paper (GB002, 4 in. × 5-1/4 in., Schleicher & Schuell) were hydrated in 1 M ammonium acetate prior to assembly on a Minifold I (Schleicher and Schuell). The Minifold I dot blot apparatus was modified as previously described by Wong and Lohman [47]. Vacuum was applied to the apparatus such that the filtration rate of 1 M ammonium acetate was ~1 ml/min. Samples (400 μl, 100 ng) were applied to the membrane in duplicate, allowed to vacuum filter, and washed immediately with 500 μl of 1 M ammonium acetate. Directly after the wash step, the membrane was removed from the manifold and subjected to UV-light crosslinking in a Stratalinker 1800 set to auto crosslink (~0.12 J/cm^2). Following the photocrosslinking reaction, the membrane was incubated with gentle agitation in 20 ml of 1× casein TBS solution (Vector Laboratories) for 30 min. The blocking solution was then replaced with 20 ml of fresh 0.2× casein TBS solution containing 0.05% Tween 20 and streptavidin-horseradish peroxidase conjugate (1 μg) was added, and the incubation continued for 60 min. After removing the streptavidin-horseradish peroxidase solution, the membrane was washed five times with casein TBS solution. Following the last wash step, the membrane was incubated with 2 ml of SuperSignal Westfemto chemiluminescent reagent for 3 min. Excess SuperSignal reagent was removed and the chemiluminescence was quantified using a ChemiGenius^{2XE} digital imaging instrument (SynGene) with the exposure time set to 4 min.

NIH-PA Author Manuscript

NIH-PA Author Manuscript

NIH-PA Author Manuscript

2.7. Two-dimensional thin-layer chromatography

CJ236 DNA (20 μg), purified from cultures (10 ml) supplemented with 25 μCi/ml of ^{32}P orthophosphoric acid or [6-^{3}H]uracil, was hydrolyzed to 2′-deoxynucleoside 5′-monophosphates in reactions (100 μl) containing DNase I (2.3 U) and snake venom phosphodiesterase (0.042 U) in buffer B (50 mM Tris–HCl (pH 8.0), 50 mM NaCl, 5 mM $MgCl_2$) conducted at 37 °C for 20 min. Reactions were evaporated to near dryness in a Speedy Vac and resuspended in 50 μl of dH_2O. A polyethyleneimine-cellulose (PEI-cellulose) sheet (J.T. Baker) was spotted approximately 2 cm from the bottom edge with 5 μl of the ^{32}P hydrolysate, allowed to dry, and then soaked in methanol for 5 min as described by Bochner and Ames [48]. After drying, the PEI-cellulose chromatogram was placed in a glass solvent tank containing 1 M acetic acid brought to pH 3.5 with NaOH until the solvent front had advanced to within 1–2 cm of the top edge. The chromatogram was then soaked for 20 min in methanol, air-dried, rotated 90° counterclockwise, and placed in a solvent tank containing 5.6 M ammonium sulfate, 35 mM ammonium hydrogen sulfate, and 0.12 M EDTA, pH adjusted to 3.5 with NaOH, until the solvent front reached the top of the sheet. Autoradiography of the dried ^{32}P chromatogram was performed using Kodak BioMax MS film. The PEI-cellulose sheets were then imaged by epi-UV light and the 2′-deoxynucleoside 5′-monophosphate spots were cut out, scraped into a scintillation vials, and counted for radioactivity in a Beckman LS6500.

2.8. Mass spectrometric analysis of CJ236 DNA

CJ236 early log DNA (20 μg) was hydrolyzed to 2′-deoxynucleosides in reactions (100 μl) containing DNase I (4.6 U), snake venom phosphodiesterase (0.084), and shrimp alkaline phosphatase (2 U) and buffer B. After digestion at 37 °C for 45 min, the hydrolysates were passed through a 3000 MWCO centrifugal filter before determining the deoxynucleoside concentration spectrophotometrically. The digested DNA was diluted 1:1 in distilled water, and 50 μl were analyzed by LC/MS using a PE Sciex API 365 triple quadrupole mass spectrometer with a Shimadzu CBM-20A HPLC equipped with a Phenomenex 4u Hydro-RP 80A 2.1 mm × 150 mm 4 μm column. An isocratic solvent system was employed that consisted of 0.1% acetic acid:10% MeOH at 0.1 ml/min flow rate. Multiple reaction monitoring analysis of two transitions (500 ms/transition) was conducted: for dUrd, 229–113 *m/z*, and for dThd, 243–127 *m/z*.

3. Results

3.1. Scheme for detection of uracil residues in DNA

A scheme of the method used here for detection of uracil residues in DNA is presented in Fig. 1. In order to construct a uracil-DNA standard, double-stranded M13 mp2 DNA that contained a site-specific U·A base pair was prepared by annealing a uracil-containing oligodeoxynucleotide to single-stranded M13 DNA and conducting a primer extension reaction as previously described [45]; this M13 U·A DNA contained one uracil residue per 14,392 nt. First, the M13 U·A standard DNA and a highly purified sample of the unknown DNA to be analyzed were pre-treated in separate reactions with Nfo, Pol β 8 kDa domain dRPase, and methoxyamine (MX) in order to remove ARP-reactive sites. Second, the M13 U·A standard DNA was reacted with Ung to create an abasic or AP-site. The AP-site was then cleaved by T4pdg, leaving a highly reactive 3′-α,β-unsaturated aldehyde which rapidly combined with ARP to produce a stable 3′-4-hydroxy-2-pentenal ARP oxime [49]. In this fashion each uracil residue was replaced with an ARP moiety containing a biotin. In a control reaction, the pre-treated unknown DNA was combined with ARP and T4pdg but not Ung, in order to determine the background level of ARP-DNA adduction in the absence of uracil excision. The M13 U·A standard DNA and control unknown DNA were combined in various ratios to produce uracil-DNA standards that contained from one uracil per million

NIH-PA Author Manuscript

NIH-PA Author Manuscript

NIH-PA Author Manuscript

nucleotides (1 U/10^6 nt) to 16 U/10^6 nt. The uracil-DNA standards were applied to a nitrocellulose membrane using a dot blot vacuum manifold, and the membrane was blocked, incubated with streptavidin conjugated to horseradish peroxidase, developed with chemiluminescence substrate and imaged in a ChemiGenius^{2XE} digital imaging system.

3.2. Uracil-DNA standard curve

A standard curve for detection of uracil residues in DNA is shown in Fig. 2A. Increasing amounts of ARP-treated M13 U·A DNA containing 0–16 uracil residues per 10^6 DNA nt (U/10^6 nt) were applied to a nitrocellulose membrane, which was developed as described above and visualized by chemiluminescence. The chemiluminescence of the individual uracil-DNA standards increased in a linear fashion with respect to the amount of uracil in the samples. Mock-treated bacterial DNA was added to the M13 U·A DNA samples to control for the level of chemiluminescence produced by non-uracil related ARP adduction in the analyte DNA (Fig. 2B). This “background” chemiluminescence represented 10% of the chemiluminescence produced by the 16 U/10^6 nt uracil-DNA standard. To determine the extent to which uracil-DNA-associated chemiluminescence remained linear, increasing amounts of uracil-rich DNA from the *E. coli* strain CJ236 (see Section 3.6) were analyzed (Fig. 2C). The results show that the linear range of the chemiluminescence reaction extended to at least 80 U/10^6 nt (Fig. 2C).

3.3. Uracil accumulation in isogenic E. coli ung/dug mutant strains

In order to determine the contribution of Ung and Dug/Mug to uracil avoidance in *E. coli* DNA, we constructed *ung* and *dug* mutants of the parental strain, JM105 [39], using P1-mediated generalized transduction of transposon-encoded drug resistance gene insertions [44] as described under Section 2. Three mutant strains were created from JM105 (*ung*$^+$ *dug*$^+$): CY01 (*dug*), CY10 (*ung*), and CY11 (*ung dug*). The mutant genotypes were verified by acquired drug resistance, PCR, and activity assays (data not shown). Genomic DNA from the four strains was extracted from cultures at early log or saturated phase growth and analyzed for uracil using the Ung-ARP assay (Fig. 3). The limit of detection using the uracil-DNA standard curve was 1 U/10^6 (Fig. 3A). The intensity of uracil-dependent chemiluminescence was not the limiting factor; rather, the sensitivity of the assay was limited by the chemiluminescence emitted by the control DNA (see Fig. 1). This “background” chemiluminescence (0.36 units) was ARP-dependent but not Ung-dependent; the chemiluminescence of the 1 U/10^6 nt standard was 0.5 units (Fig. 3).

DNA from early log and saturated cultures of JM105 and CY01 did not contain uracil above the limit of detection. This observation indicates that the absence of the *dug* gene product alone did not result in increased uracil-DNA. However, DNA from CY10, the *ung* mutant strain, in early log growth phase contained 31 U/10^6 nt (Fig. 3B). Thus, disruption of the *ung* gene resulted in more than a 30-fold increase in uracil-DNA. The amount of uracil in DNA isolated from saturated phase growth CY10 cultures was determined to be 19 U/10^6 nt. Similarly, DNA from CY11, which is mutant for *ung* and *dug*, contained 33 U/10^6 nt when extracted from cultures in early log phase growth, and 23 U/10^6 nt from cultures in late log growth. These results indicate that disruption of *dug* in strains already mutant in *ung* did not measurably increase the level of uracil-DNA. For both CY10 and CY11, uracil accumulation decreased in saturated phase growth.

3.4. Effect of 5-fluorouridine supplementation on uracil levels in CY11 (ung dug)

The use of fluoropyrimidine antimetabolites such as 5-fluorouracil (5-FU) and 5-fluorodeoxyuridine (5-FdUrd) in cancer treatment is widespread. These analogs are converted intracellularly to 5-FdUMP, which forms a stable inhibitory complex with thymidylate synthase and 5,10-methylene-tetrahydrofolate [50], and irreversibly blocks the

NIH-PA Author Manuscript

NIH-PA Author Manuscript

NIH-PA Author Manuscript

de novo synthesis of dTMP. As a result of diminished dTTP pools, DNA replication is inhibited and cellular DNA becomes fragmented. At sufficiently high doses, 5-FU and 5-FdUrd exert cell-killing effects.

In order to quantify the effect of 5-FdUrd supplementation on the accumulation of uracil in *E. coli* DNA, we diluted overnight cultures of the uracil-DNA glycosylase-defective *ung dug* mutant CY11 into fresh minimal medium containing 0, 10, or 20 ng/ml of 5-FdUrd, isolated the genomic DNA at early log and saturated phase growth, and probed for uracil residues using the Ung-ARP assay (Fig. 4). In the absence of 5-FdUrd supplementation, early log phase CY11 DNA contained 31 ± 1 U/10^6 nt (Fig. 4, lane 1), in good agreement with the measurement presented in Fig. 3B, lane 7 (33 U/10^6 nt). When propagated in the presence of 10 ng/ml 5-FdUrd, the concentration of uracil in early log phase CY11 DNA increased to 101 ± 8 U/10^6 nt, and in the presence of 20 ng/ml 5-FdUrd, the uracil concentration was 125 ± 2 U/10^6 (Fig. 4, lanes 2 and 3, respectively). At 5-FdUrd concentrations of 50 ng/ml and higher, CY11 cells grew poorly or not at all (data not shown). Thus, treatment of CY11 cells with 10–20 ng/ml of 5-FdUrd resulted in a respective 3.3- to 4-fold increase over untreated cells in the amount of uracil in early log phase growth genomic DNA. However, analysis of CY11 DNA from the saturated growth phase showed that the effect of 5-FdUrd on uracil levels was largely absent (Fig. 4, lanes 4–6). The level of uracil in untreated CY11 DNA at saturated growth phase was found to be 24 ± 5 U/10^6 nt, in agreement with the earlier measurement of 23 ± 5 U/10^6 presented in Fig. 3, lane 8. In CY11 treated with 10 or 20 ng/ml 5-FdUrd, analysis of saturated phase DNA revealed the levels of uracil to be 25 ± 5 and 32 ± 3 U/10^6 nt, respectively (Fig. 4, lanes 5 and 6). Lastly, when the uracil-DNA glycosylase-proficient strain JM105 (*ung*$^+$ *dug*$^+$) was treated with 10 and 20 ng/ml of 5-FdUrd, no increase in uracil was observed in DNA extracted from either early log or saturated growth phase (data not shown).

3.5. Effect of nucleoside supplementation on uracil accumulation

E. coli cells are capable of producing *de novo* sufficient quantities of nucleoside precursors for DNA and RNA synthesis; however, externally supplied nucleosides can also be utilized via the salvage pathway and may even serve as a sole carbon or nitrogen source [51]. Interestingly, it was reported that wild type *E. coli* cells did not normally utilize exogenous thymine, presumably because they lacked an adequate 2′-deoxyribose-1-phosphate pool [52,53]. Exogenous thymidine was reported to be poorly incorporated into *E. coli* DNA because thymidine phosphorylase (*deoA*), which is inducible, degraded the thymidine to thymine [52]. In order to determine the effect of pyrimidine nucleosides on uracil accumulation in CY11 (*ung dug*), which is wild type for thymidylate synthase (*thyA*) and the *de novo* pathway for dTTP synthesis, we supplemented cultures of CY11 in minimal medium with 100 μg/ml of either deoxyuridine, thymidine, uridine, or a combination of thymidine and uridine, or not at all (control cultures). Genomic DNA was then extracted from CY11 early log or saturated growth phase cultures and subjected to the Ung-ARP assay (Fig. 5). Addition of thymidine to early log cultures resulted in DNA that contained 34 ± 2 U/10^6 nt and was essentially undistinguishable from that of the CY11 control culture, which contained 31 ± 1 U/10^6 nt, in agreement with previous measurements (see Figs. 3 and 4). Similarly, DNA from CY11 cultures supplemented with uridine contained 31 ± 1 U/10^6 nt. However, CY11 DNA isolated from early log cultures supplemented with 100 μg/ml deoxyuridine had a significantly lower level of uracil, 8 ± 0.3 U/10^6 nt (Fig. 5A, lane 2). The effect of deoxyuridine supplementation on reduced uracil incorporation persisted in DNA isolated from CY11 cells in saturated growth phase, which contained 7 ± 0.1 U/10^6 nt (Fig. 5B, lane 2). The combination of thymidine and uridine supplementation also resulted in a lower level of uracil incorporation, as DNA from early log and saturated growth phases contained 13 ± 0.4 and 10 ± 0.5 U/10^6 nt, respectively. Overall, the level of uracil

NIH-PA Author Manuscript

NIH-PA Author Manuscript

NIH-PA Author Manuscript

incorporation declined under saturated growth conditions. For example, DNA from control CY11 cultures in saturated phase contained 21 ± 0.3 U/10^6 nt compared to 31 ± 1 U/10^6 nt for early log phase; levels of uracil in DNA from thymidine-or uridine-supplemented cultures followed a similar trend (Fig. 5).

3.6. Uracil accumulation in CJ236 (dut-1 ung-1) DNA

In *E. coli*, a considerable amount of dUTP is produced since it is an obligatory intermediate in the *de novo* synthesis of dTMP [23]. Although the DNA polymerases of *E. coli* do not effectively discriminate dUTP from dTTP, little dUTP finds its way into *E. coli* DNA because of the action of dUTP pyrophosphatase, which hydrolyzes dUTP to dUMP and PP_i [10]. In early studies of *dut* mutants, it was anticipated that the *dut* mutant DNA would contain uracil [10]; however, the nascent DNA of these mutants was found to be exceptionally fragmented [3]. Such fragmentation was consistent with the excision of transiently incorporated uracil by uracil-DNA glycosylase (Ung) and subsequent incision of the Ung-generated abasic sites by apurinic/apyrimidinic endonuclease [23]. Inactivation of the *ung* gene permitted stable incorporation of uracil into the DNA of *dut* mutants [8].

The *E. coli* strain CJ236 (*dut-1 ung-1*) has reduced dUTP pyrophosphatase activity and no uracil-DNA glycosylase (Ung) activity, and has been used effectively for preparing uracil-containing M13 DNA templates [54]. CJ236 was constructed by C. Joyce (Yale University) from an isolate of BW313 (Hfr KL16 (PO-45) *dut-1 ung-1 thi-1 relA1 spoT1; personal communication*, B. Weiss, Emory University) that had spontaneously lost the Hfr phenotype by introducing a selectable F′ (pCJ105) [54]. Weiss and co-workers demonstrated that a *dut* null mutation was lethal, even in an *ung* background [23]; therefore, viable *dut* mutations are missense mutations. CJ236 was propagated at 25–30 °C in the presence of 125 μg/ml thymidine in order to avoid creation of secondary mutations, and checked for thymidine auxotrophy by plating at 42 °C as noted by el-Hajj et al. [23] and B. Weiss (personal communication). In order to identify the *dut* mutation(s) in CJ236, we amplified the *dut* gene in purified CJ236 genomic DNA using PCR and sequenced the PCR product as described under Section 2. The results show that the CJ236 *dut* mutation consists of a single nucleotide change, a C→T transition mutation at position 71 of *E. coli dut* coding sequence [55] which generates a Thr→Ile amino acid change at codon 24. These results agree with those reported by Kouzminova and Kuzminov [56] for the *dut-1* allele of *E. coli* PK4001 constructed by Steiner and Kuempel [57].

Having verified the mutant *dut* gene status in CJ236 by DNA sequencing, we subjected CJ236 DNA purified from early log cultures grown at 30 °C in minimal medium to the Ung-ARP assay (Fig. 6). Preliminary determinations indicated that uracil accumulation in CJ236 DNA reached 1000 U/10^6 nt. Although this level represented a 30-fold increase over the amount of uracil found in CY11 (*ung dug*), it was substantially lower than uracil-DNA levels reported previously for *dut ung* mutants [8,25]. However, it should be noted that *dut* mutants vary widely in residual dUTP pyrophosphatase activity [4], and the actual mutations in these *dut* strains and the occurrence of secondary mutations (i.e. *deoA*) were not determined. We hypothesized that if the level of uracil in CJ236 were actually several-fold higher, then Ung, the *E. coli* uracil-DNA glycosylase used in the Ung-ARP reaction, might have been subject to product (AP-site) inhibition.

Uracil-DNA glycosylase generates two reaction products: free uracil and apyrimidinic DNA; however, apyrimidinic-sites inhibit uracil-DNA glycosylase activity at concentrations 100–1000-fold lower than uracil [58,59]. Therefore, to reduce AP-site product inhibition, we increased the ratio of Ung enzyme to CJ236 DNA in the Ung-ARP reaction by holding the amount of Ung constant (0.2 units) and decreasing the amount of CJ236 DNA from 10 to 1 μg. Following the Ung-ARP reaction, samples of the ARP-labeled CJ236 DNA (0.4 and 0.8

NIH-PA Author Manuscript

NIH-PA Author Manuscript

NIH-PA Author Manuscript

ng) were combined with JM105 control DNA and applied to a dot blot membrane as described under Section 2. As shown in Fig. 6B, the chemiluminescence of CJ236 DNA reacted in 1 μg amounts corresponded to 2915 U/10^6 nt, a level of uracil three-fold higher than the original 10 μg determination (Fig. 6C). To further investigate whether product inhibition of Ung was relieved by lower amounts of uracil-rich CJ236 DNA, we reduced the amount of CJ236 DNA in the Ung-ARP reaction to 0.1 μg. The chemiluminescence of these samples (Fig. 6B) corresponded to 3005 U/10^6 nt, essentially equal to the determination made using 1 μg of CJ236 DNA. Therefore, we concluded that the initial determinations of uracil levels were low because Ung had been inhibited by the high concentration of AP-sites, and that the actual amount of uracil in CJ236 DNA was 3000 U/10^6 nt.

3.7. Determination of uracil in CJ236 DNA by 2D thin-layer chromatography

Cellular nucleotides have been separated successfully by thin-layer chromatography using polyethyleneimine-cellulose (PEI-cellulose) sheets [48]. Therefore, to corroborate the level of uracil residues in CJ236 as determined by the Ung-ARP assay, we supplemented exponentially growing cultures of CJ236 with $^{32}P_i$ and isolated the genomic DNA as described under Section 2. The ^{32}P CJ236 DNA was then hydrolyzed enzymatically to ^{32}P 2′-deoxynucleoside 5′-monophosphates which were applied to PEI-cellulose sheets and separated in two dimensions as described by Steinberg and co-workers [60]; nonradioactive dUMP was added to the ^{32}P DNA digest prior to analysis as a marker for ^{32}P dUMP.

The DNA ^{32}P 2′-deoxynucleoside 5′-monophosphates were separated using two solvent systems. The first dimension solvent consisted of 1 M acetic acid adjusted to pH 3.5 with NaOH, and the second dimension solvent was prepared from ammonium sulfate, ammonium hydrogen sulfate, and EDTA, and also adjusted to pH 3.5 with sodium hydroxide [60]. Following chromatography, the cellulose sheets were placed on X-ray film overnight and then imaged using the fluorescence mode of a ChemiGenius^{2XE} digital imager. When illuminated with 254 nm light, the 2′-deoxynucleoside 5′-monophosphates appeared as black spots against the light fluorescent green background of the PEI-cellulose sheet (Fig. 7A). After chromatography in the 1st dimension, dUMP migrated farthest, followed by dCMP, dTMP, dGMP, and dAMP, respectively. The PEI-cellulose sheet was rotated 90° counterclockwise, and the second dimension solvent front was allowed to migrate to the end of the sheet; this step effectively separated the pyrimidine ^{32}P 2′-deoxynucleoside 5′-monophosphates. An autoradiogram of the final chromatogram is shown in Fig. 7B.

The spots corresponding to the various ^{32}P dNMPs were cut out from the PEI-cellulose sheet and counted for ^{32}P radioactivity in a liquid scintillation spectrometer (Table 1). The results from four independent experiments showed that incorporation of $^{32}P_i$ into CJ236 DNA was asymmetric with respect to the four conventional 2′-deoxynucleoside 5′-monophosphates. dGMP contained the most ^{32}P radioactivity, accounting for almost 36% of total detected ^{32}P counts, whereas dTMP contained the least, 17.2%. Significantly, in CJ236 DNA dUMP represented 0.66% of total ^{32}P radioactivity detected. This fraction is equivalent to a level of uracil per million nucleotides of 6644 (Table 1). The ratio of ^{32}P cpm detected in dUMP to the sum of ^{32}P cpm detected in dUMP and dTMP was 0.0372, which corresponds to 1 uracil residue per 26 thymine residues, given that dTMP occurs with equal frequency in genomic DNA as the other deoxynucleotides.

In a separate experiment, a culture of CJ236 was supplemented with [6-^{3}H]uracil and hydrolyzed to 2′-deoxynucleoside 5′-monophosphates as described above. The digest was then supplemented with cold dNMPs, subjected to two-dimensional thin-layer chromatography, and the spots corresponding to the five dNMPs were counted for ^3H radioactivity (Table 2). Interestingly, the largest amount of ^3H radioactivity, 64.7%, was detected in dCMP spots. In contrast, the amount of ^3H radioactivity detected in dTMP and

NIH-PA Author Manuscript

NIH-PA Author Manuscript

NIH-PA Author Manuscript

dUMP spots accounted for 31.6 and 2.56%, respectively. The ratio of ^{3}H cpm in dUMP to the sum of ^{3}H dUMP plus ^{3}H dTMP was 0.0754, which corresponds to 1 uracil residue per 12 thymine residues or 18,850 U/10^{6} nt.

3.8. Determination of uracil in CJ236 DNA by LC/MS mass spectrometry

Samples of purified CJ236 DNA were digested to deoxynucleosides by a combination of DNase I, snake venom phosphodiesterase I, and shrimp alkaline phosphatase, passed through a 3000 MWCO centrifugal filter (Microcon), and analyzed using a Sciex triple quadrupole mass spectrometer as described under Section 2. In LC mode, deoxyuridine and deoxythymidine were well separated by reverse phase chromatography, and MRM mass spectrometric identification of the constituent nucleobases verified the ratio of the two deoxynucleosides. The results, shown in Table 3, indicate that the ratio of deoxyuridine to deoxythymidine in CJ236 DNA was 0.0320 ± 0.004, which corresponds to 1 uracil residue per 31 thymine residues or 7752 U/10^{6} nt.

4. Discussion

In this report, the influence of the *ung*, *dug*, and *dut* genes in preventing uracil residues from accumulating in *E. coli* DNA was quantitatively determined using a novel assay, the Ung-ARP assay. We found that inactivation of the *ung* gene in CY10 resulted in a more than 30-fold increase in the level of uracil-DNA, whereas inactivation of *dug* had no measurable effect. Uracil levels in the DNA of CY11, an *ung dug* mutant, were not significantly higher compared to the *ung* mutant. Inactivation of *ung* and defective *dut* in the *E. coli* strain CJ236 resulted in a 100-fold increase in levels of uracil-DNA compared to the inactivation of *ung* alone in CY10.

We observed that a *dug* mutation in an *ung*$^{+}$ background had no detectable effect on uracil levels relative to the wild type strain (Fig. 3). This result was consistent with the report by Mokkapati et al. [17] which concluded that Ung and Dug process different lesions *in vivo*. Since extracts of *ung dug* strains lack detectable uracil-initiated BER [16], it would appear that Ung and Dug are the sole activities in *E. coli* capable of removing uracil from DNA. Thus, use of CY11 allows determination of the amount of uracil that escaped cleavage by dUTP pyrophosphatase and was incorporated into nascent DNA under various growth conditions [3].

We consistently observed that the level of uracil in DNA extracted from saturated cultures of CY11 was lower than that from early log cultures (Fig. 3B). This reduction may result from slowing of cell division as the cell density of the culture reaches a critical level and nutrients become limiting. Longer periods between replication cycles may give dUTP pyrophosphatase more time to sanitize DNA precursor pools. In addition, as *E. coli* cultures approach saturation, some cells die and release their contents, which include nucleosides and nucleotides, into the culture medium. These compounds can be utilized by salvage pathways in living cells to supplement dTMP pools.

Levels of uracil in CY11 cells treated with 5-fluoro-2′-deoxyuridine declined in saturated phase (Fig. 4). One possible explanation for this decline is that the amount of 5-fluoro-2′-deoxyuridine in the medium was nearly depleted in saturated phase cultures. Summers and Raksin [61] found that by supplementing the culture medium with adenine, guanosine, cytidine, and uridine, single-step resistance to 5-fluoro-2′-deoxyuridine (50 μM) could be obtained by inactivation of the gene for thymidine kinase, *tdk*. While we did not look for *tdk* or *deoA* mutations in CY11 grown in the presence of 5-fluoro-2′-deoxyuridine, we note that the amount of 5-fluoro-2′-deoxyuridine (50 μM = 12.3 μg/ml) used by Summers and Raksin

NIH-PA Author Manuscript

NIH-PA Author Manuscript

NIH-PA Author Manuscript

to induce *tdk* mutation was 615-fold greater than the highest concentration used in this investigation.

Addition of deoxyuridine to CY11 cultures led to a significant decline in the amount of uracil-DNA (Fig. 5). Deoxyuridine effectively induces the *deo* operon and is efficiently degraded to uracil and deoxyribose 1-phosphate by the *deoA* gene product, thymidine phosphorylase; a minor percentage of deoxyuridine is phosphorylated to dUMP by thymidine kinase and available for methylation by thymidylate synthase [62]. Since deoxyuridine acts a competitive inhibitor of thymine phosphorylase-mediated cleavage of thymidine, more thymidine is available for phosphorylation to dTMP. In addition, expansion of the deoxyribose 1-phosphate pool enables production of thymidine from endogenous thymine in a synthetic reaction catalyzed by thymidine phosphorylase [62]. The dUTP pool is probably reduced by deoxyuridine supplementation, since the increase in the dTTP pool inhibits dCTP deaminase, an important contributor to the dUTP pool [10]. Uridine can not serve as a source of deoxyribose 1-phosphate, and thymidine is rapidly broken down to thymine and deoxyribose 1-phosphate, which in turn is degraded by phosphodeoxyribomutase (*deoB*) and phosphodeoxyriboaldolase (*deoC*). As observed by Budman and Pardee [52] and here in Fig. 5, incorporation of exogenous thymidine into DNA is increased by uridine, presumably because uridine competitively inhibits thymidine phosphorylase and prevents its induction by thymidine.

DNA sequencing of the CJ236 gene revealed that the defective dUTP pyrophosphatase activity in this strain was the result of a Thr24Ile amino acid change. In the crystal structure of *E. coli* dUTP pyrophosphatase solved by Barabas et al. [63], the oxygen atom of the Thr24 side chain (Thr25 as shown in Fig. 8) shares a hydrogen bond with a water molecule that is hydrogen-bonded to a carboxylate oxygen of the Asp90 side chain. Since Asp90 is responsible for coordinating the water molecule (Wcat in Fig. 8) that initiates the nucleophilic attack on the α-phosphorus atom of dUTP, it important that the Asp90 side chain be maintained in the correct position, and the Thr25 oxygen contributes indirectly to this task. Substitution of Thr24 with Ile introduces an apolar residue at this position, which apparently is poorly tolerated in terms of enzyme activity. While Thr24 is not strictly conserved in dUTP pyrophosphatases, an apolar residue has not been found at this sequence position [64]. This observation argues for the importance of polar/charged character at this location in the enzyme/substrate structure. In eukaryotic dUTP pyrophosphatase, the position equivalent to Thr24 is occupied by Ser, whereas in viral enzymes, either Thr or Ser is found. Mutation of Thr24 in *E. coli* dUTP pyrophosphatase to a polar residue such a His (as occurs in Mycobacteria), which is also capable of hydrogen bonding, may result in retention of enzyme activity by some rearrangement around the Asp90 side chain.

AP-sites inhibit uracil-DNA glycosylase because the enzyme binds more tightly to the AP-site reaction product than to uracil-DNA [59,65]. Thus, when our initial determination of the amount of uracil in CJ236 (*dut-1ung-1*) DNA by the Ung-ARP assay appeared low (1000 U/10^6 nt), we suspected that Ung was AP-site inhibited and increased the Ung:uracil-DNA molar ratio by reducing the amount of substrate DNA and holding the amount of enzyme constant. Reducing the amount of CJ236 DNA in the assay 10- and 100-fold produced results that were in close agreement: 2915 and 3005 U/10^6 nt, respectively. AP-site inhibition of Ung by other DNAs, such as CY11 (*ung dug*), was not observed (data not shown).

Blount and Ames [25] reported that *E. coli* CJ236, propagated at 37 °C, contained 1.22% uracil residues by weight, as determined by HPLC reverse chromatography and UV absorbance. We calculate that 1.22% uracil by weight is equivalent to 12.2 μg uracil per mg of DNA, 14% replacement of T by U, or ~35,000 U/10^6 nt. In a subsequent report, Atamna

NIH-PA Author Manuscript

NIH-PA Author Manuscript

NIH-PA Author Manuscript

et al. [30] determined by GC/MS that the amount of uracil in CJ236 DNA was actually 0.28%, which we calculate to be ~8000 U/10^6 nt. The effect of temperature on dUMP incorporation in an *E. coli dut ung* strain was investigated by Warner and co-workers, who propagated BD1157 (*dut-1 ung-1*) at different temperatures in the presence of [6-^{3}H]uridine [8]. By interpolation of their graphical data, we estimate that replacement of thymine with uracil in BD1157 DNA increased from 5% at 30 °C to over 12% at 37 °C [8]. Thus, the amount of uracil in *E. coli dut-1* DNA can vary considerably depending on the growth temperature.

We also determined the uracil content of CJ236 DNA by thin-layer chromatography of *in vivo* ^{32}P- or [6-^{3}H]uracil-labeled CJ236 2′-deoxyribose 5′-monophosphates as well as by LC/MS of deoxyuridine and thymidine 2′-deoxynucleosides (Tables 1–3). Examination of the ^{32}P data showed that, based on the total ^{32}P radioactivity detected, the amount of ^{32}P dUMP observed corresponded to 6644 ± 1179 U/10^6 nt. However, the ratio of ^{32}P dUMP to the sum of ^{32}P dUMP + ^{32}PdTMP, 0.0372, indicated that level of uracil was 9300 ± 725 U/10^6 nt. The reason for this disparity is not clear; however, it is apparent the distribution of ^{32}P radioactivity in spots corresponding to dAMP, dCMP, dGMP, and dTMP was skewed toward dGMP, which represented almost 36% of total ^{32}P cpm. Analysis of [6-^{3}H]uracil-labeled CJ236 showed that the ratio of ^{3}H dUMP to the sum of ^{3}H dUMP + ^{3}H dTMP was 0.0754, which, upon extrapolation, corresponds to 18,850 U/10^6 nt (Table 2). This determination of uracil levels in CJ236 DNA was about twofold higher than that obtained with $^{32}P_i$ labeling, most likely because the dUTP pool was increased by [6-^{3}H]uracil supplementation through the action of the pyrimidine salvage pathway [66].

Using LC/MS we found that the U to T ratio was 0.032, which was equivalent to 7752 U/10^6 nt (Table 3). Given that labeling with [6-^{3}H]uracil may have produced artifactually high U:T ratios, the average level of uracil residues in CJ236 DNA detected by $^{32}P_i$ labeling and LC/MS was 7899 U/106 nt, compared to 3000 U/10^6 nt by the Ung-ARP assay, a ~2.5-fold difference. We speculate that the extremely high concentration of uracil residues in *dut*-defective bacteria like CJ236 DNA may have been underestimated by the Ung-ARP assay because (1) not all uracil residues may have been accessible for excision by uracil-DNA glycosylase, and (2) not all the biotin-tagged sites in the DNA deposited on the nitrocellulose membrane were accessible to streptavidin binding.

Recent measurements of uracil levels in the DNA of folate-deficient human beings range from 4.6 μmol U/mol DNA (4.6 U/10^6 nt) [29] to 34,600–167,000 uracils/diploid cell [67] to 500,000–4,000,000 uracils/diploid cell (83.3–667 U/10^6 nt) [32]. Since the reproducibility of the Ung-ARP assay for uracil levels in the low to medium range was excellent, we propose that this method is well suited for determining the level of uracil residues in human cells.

Acknowledgments

We are grateful to Dr. Bernie Weiss (Emory University) for his generous gifts of bacterial strains and insightful comments. We acknowledge the Mass Spectrometer Facility of the Environmental Health Science Center (Grant P30 ES00210) at Oregon State University for mass spectrometric analyses.

References

1. Tye BK, Chien J, Lehman IR, Duncan BK, Warner HR. Uracil incorporation: a source of pulse-labeled DNA fragments in the replication of the *Escherichia coli* chromosome. Proc Natl Acad Sci USA 1978;75:233–237. [PubMed: 203931]
2. Mosbaugh DW, Bennett SE. Uracil-excision DNA repair. Prog Nucl Acid Res Mol Biol 1994;48:315–370.

NIH-PA Author Manuscript

NIH-PA Author Manuscript

NIH-PA Author Manuscript

3. Tye B-K, Nyman P-O, Lehman IR, Hochhauser S, Weiss B. Transient accumulation of Okazaki fragments as a result of uracil incorporation into nascent DNA. Proc Natl Acad Sci USA 1977;74:154–157. [PubMed: 319455]
4. Hochhauser SJ, Weiss B. *Escherichia coli* mutants deficient in deoxyuridine triphosphatase. J Bacteriol 1978;134:157–166. [PubMed: 148458]
5. O'Donovan, GA. Thymidine Metabolism in Bacteria. Plenum Publishing; New York: 1977. p. 219-253.
6. Bessman MJ, Lehman IR, Adler J, Zimmerman S, Simms ES, Kornberg A. Enzymatic synthesis of deoxyribonucleic acid. III. The incorporation of pyrimidine and purine analogues into deoxyribonucleic acid. Proc Natl Acad Sci USA 1958;44:633–640. [PubMed: 16590253]
7. Mosbaugh DW. Purification and characterization of porcine liver DNA polymerase gamma: utilization of dUTP and dTTP during *in vitro* DNA synthesis. Nucl Acid Res 1988;16:5645–5659.
8. Warner HR, Duncan BK, Garrett C, Neuhard J. Synthesis and metabolism of uracil-containing deoxyribonucleic acid in *Escherichia coli*. J Bacteriol 1981;145:687–695. [PubMed: 6109711]
9. Shlomai J, Kornberg A. Deoxyuridine triphosphatase of *Escherichia coli*. Purification, properties, and use as a reagent to reduce uracil incorporation into DNA. J Biol Chem 1978;253:3305–3312. [PubMed: 346589]
10. Wang L, Weiss B. *dcd* (dCTP deaminase) gene of *Escherichia coli*: mapping, cloning, sequencing, and identification as a locus of suppressors of lethal *dut* (dUTPase) mutations. J Bacteriol 1992;174:5647–5653. [PubMed: 1324907]
11. Bertanie LE, Haggmark A, Reichard P. Synthesis of pyrimidine deoxyribonucleoside diphosphates with enzymes from *Escherichia coli*. J Biol Chem 1961;236:PC67–PC68. [PubMed: 13868387]
12. Bertanie LE, Haggmark A, Reichard P. Enzymatic synthesis of deoxyribonucleotides. II. Formation and interconversion of deoxyuridine phosphates. J Biol Chem 1963;238:3407–3413. [PubMed: 14085395]
13. Weiss B, Wang L. De novo synthesis of thymidylate via deoxycytidine in dcd (dCTP deaminase) mutants of *Escherichia coli*. J Bacteriol 1994;176:2194–2199. [PubMed: 8157589]
14. Lindahl T. DNA glycosylases, endonucleases for apurinic/apyrimidinic sitesand base excision-repair. Prog Nucl Acid Res Mol Biol 1979;22:135–192.
15. Lindahl T, Ljungquist S, Siegert W, Nyberg B, Sperens B. DNA N-glycosidases. Properties of a uracil-DNA glycosidase from *Escherichia coli*. J Biol Chem 1977;252:3286–3294. [PubMed: 324994]
16. Sung JS, Bennett SE, Mosbaugh DW. Fidelity of uracil-initiated base excision DNA repair in *Escherichia coli* cell extracts. J Biol Chem 2001;276:2276–2285. [PubMed: 11035036]
17. Mokkapati SK, de Henestrosa Fernandez AR, Bhagwat AS. *Escherichia coli* DNA glycosylase Mug: a growth-regulated enzyme required for mutation avoidance in stationary-phase cells. Mol Microbiol 2001;41:1101–1111. [PubMed: 11555290]
18. Mosbaugh DW, Linn S. Further characterization of human fibroblast apurinic/apyrimidinic DNA endonucleases. The definition of two mechanistic classes of enzyme. J Biol Chem 1980;255:11743–11752. [PubMed: 6254980]
19. Mosbaugh DW, Linn S. Characterization of the action of *Escherichia coli* DNA polymerase I at incisions produced by repair endodeoxyribonucleases. J Biol Chem 1982;257:575–583. [PubMed: 6273443]
20. Piersen CE, McCullough AK, Lloyd RS. AP lyases and dRPases: commonality of mechanism. Mutat Res 2000;459:43–53. [PubMed: 10677682]
21. Dianov G, Lindahl T. Reconstitution of the DNA base excision-repair pathway. Curr Biol 1994;4:1069–1076. [PubMed: 7535646]
22. Duncan BK, Weiss B. Specific mutator effects of *ung* (uracil-DNA glycosylase) mutations in *Escherichia coli*. J Bacteriol 1982;151:750–755. [PubMed: 7047496]
23. el-Hajj HH, Zhang H, Weiss B. Lethality of a *dut* (deoxyuridine triphosphatase) mutation in *Escherichia coli*. J Bacteriol 1988;170:1069–1075. [PubMed: 2830228]
24. Guillet M, Van Der Kemp PA, Boiteux S. dUTPase activity is critical to maintain genetic stability in *Saccharomyces cerevisiae*. Nucl Acids Res 2006;34:2056–2066. [PubMed: 16617146]

NIH-PA Author Manuscript NIH-PA Author Manuscript NIH-PA Author Manuscript

25. Blount BC, Ames BN. Analysis of uracil in DNA by gas chromatography-mass spectrometry. Anal Biochem 1994;219:195–200. [PubMed: 8080076]
26. Goulian M, Bleile B, Tseng BY. Methotrexate-induced misincorporation of uracil into DNA. Proc Natl Acad Sci USA 1980;77:1956–1960. [PubMed: 6929529]
27. Green DA, Deutsch WA. Direct determination of uracil in [^{32}P,uracil-^{3}H]poly(dA-dT) and bisulfite-treated phage PM2 DNA. Anal Biochem 1984;142:497–503. [PubMed: 6528982]
28. Duthie SJ, McMillan P. Uracil misincorporation in human DNA detected using single cell gel electrophoresis. Carcinogenesis 1997;18:1709–1714. [PubMed: 9328165]
29. Ren J, Ulvik A, Refsum H, Ueland PM. Uracil in human DNA from subjects with normal and impaired folate status as determined by high-performance liquid chromatography-tandem mass spectrometry. Anal Chem. 2001 (Web Release Date: November 29, 2001).
30. Atamna H, Cheung I, Ames BN. A method for detecting abasic sites in living cells: age-dependent changes in base excision repair. Proc Natl Acad Sci USA 2000;97:686–691. [PubMed: 10639140]
31. Liuzzi M, Talpaert-Borle M. A new approach to the study of the base-excision repair pathway using methoxyamine. J Biol Chem 1985;260:5252–5258. [PubMed: 2580833]
32. Blount BC, Mack MM, Wehr CM, MacGregor JT, Hiatt RA, Wang G, Wickramasinghe SN, Everson RB, Ames BN. Folate deficiency causes uracil misincorporation into human DNA and chromosome breakage: implications for cancer and neuronal damage. Proc Natl Acad Sci USA 1997;94:3290–3295. [PubMed: 9096386]
33. Kubo K, Ide H, Wallace SS, Kow YW. A novel, sensitive, specific assay for abasic sites, the most commonly produced DNA lesion. Biochemistry 1992;31:3703–3708. [PubMed: 1567824]
34. McCullough AK, Sanchez A, Dodson ML, Marapaka MP, Taylor JS, Lloyd RS. The reaction mechanism of DNA glycosylase/AP lyases at abasic sites. Biochemistry 2001;40:561–568. [PubMed: 11148051]
35. Sambrook, J.; Fritsch, EF.; Maniatis, T. Molecular Cloning: A Laboratory Manual. Cold Spring Harbor Laboratory; Cold Spring Harbor, NY: 1989.
36. Edlin G, Maaloe OJ. Synthesis and breakdown of messenger RNA without protein synthesis. J Mol Biol 1966;15:428–434. [PubMed: 5330747]
37. Bennett SE, Schimerlik MI, Mosbaugh DW. Kinetics of the uracil-DNA glycosylase/inhibitor protein association. J Biol Chem 1993;268:26879–26885. [PubMed: 8262921]
38. Levin JD, Johnson AW, Demple B. Homogeneous *Escherichia coli* endonuclease IV. Characterization of an enzyme that recognizes oxidative damage in DNA. J Biol Chem 1988;263
39. Yanisch-Perron C, Vieira J, Messing J. Improved M13 phage cloning vectors and host strains: nucleotide sequence of the M13mp18 and pUC19 vectors. Gene 1985;33:103–119. [PubMed: 2985470]
40. Joyce CM, Grindley ND. Method for determining whether a gene of *Escherichia coli* is essential: application to the polA gene. J Bacteriol 1984;158:636–643. [PubMed: 6233260]
41. Lutsenko E, Bhagwat AS. The role of the *Escherichia coli* mug protein in the removal of uracil and 3,N(4)-ethenocytosine from DNA. J Biol Chem 1999;274:31034–31038. [PubMed: 10521502]
42. Gallinari P, Jiricny J. A new class of uracil-DNA glycosylase related to human thymine-DNA glycosylase. Nature 1996;383:735–738. [PubMed: 8878487]
43. Sung, J-S. PhD thesis. 2002. Characterization of *Escherichia coli* double-strand uracil-DNA glycosylase and analysis of uracil-initiated base excision DNA repair.
44. Miller, JH. Experiments in Molecular Genetics. Cold Spring Harbor Laboratory Press; Cold Spring Harbor: 1972.
45. Bennett SE, Sung J-S, Mosbaugh DW. Fidelity of uracil-initiated base excision DNA repair in DNA polymerase beta-proficient and -deficient mouse embryonic fibroblast cell extracts. J Biol Chem 2001;276:42588–42600. [PubMed: 11551933]
46. Sanderson RJ, Bennett SE, Sung J-S, Mosbaugh DW. Uracil-initiated base excision DNA repair synthesis fidelity in humn colon adenocarcinoma LoVo and *Escherichia coli* extracts. Prog Nucl Acid Res Mol Bio 2001;68:165–188.
47. Wong I, Lohman TM. A double-filter method for nitrocellulose-filter binding: application to protein-nucleic acid interactions. Proc Natl Acad Sci USA 1993;90:428–432.

NIH-PA Author Manuscript

NIH-PA Author Manuscript

NIH-PA Author Manuscript

48. Bochner BR, Ames BN. Complete analysis of cellular nucleotides by two-dimensional thin layer chromatography. J Biol Chem 1982:16. [PubMed: 6273422]
49. Bennett SE, Kitner J. Characterization of the Aldehyde Reactive Probe reaction with AP-sites in DNA: influence of AP-lyase on adduct stability. Nucleos Nucl Nucl Acids 2006;25:823–842.
50. Santi DV, McHenry CS, Sommer H. Mechanism of interaction of thymidylate synthetase with 5-fluorodeoxyuridylate. Biochemistry 1974;13:471–481. [PubMed: 4203910]
51. Zhang Y, Craig JE, Gallagher MP. Location of the nupC gene on the physical map of *Escherichia coli* K-12. J Bacteriol 1992;174:5758–5759. [PubMed: 1512211]
52. Budman DR, Pardee AB. Thymidine and thymine incorporation into deoxyribonucleic acid: inhibition and repression by uridine of thymidine phosphorylase of *Escherichia coli*. J Bacteriol 1967;94:1546–1550. [PubMed: 4862197]
53. Ahmad SI, Kirk SH, Eisenstark A. Thymine metabolism and thymineless death in prokaryotes and eukaryotes. Annu Rev Microbiol 1998;52
54. Kunkel TA, Roberts JD, Zakour RA. Rapid and efficient site-specific mutagenesis without phenotypic selection. Meth Enzymol 1987;154:367–382. [PubMed: 3323813]
55. Lundberg LG, Thoresson HO, Karlstrom OH, Nyman PO. Nucleotide sequence of the structural gene for dUTPase of *Escherichia coli* K-12. EMBO J 1983;2:967–971. [PubMed: 6139280]
56. Kouzminova EA, Kuzminov A. Chromosomal fragmentation in dUTPase-deficient mutants of *Escherichia coli* and its recombinational repair. Mol Microbiol 2004;51:1279–1295. [PubMed: 14982624]
57. Steiner WW, Kuempel PL. Sister chromatid exchange frequencies in *Escherichia coli* analyzed by recombination at the dif resolvase site. J Bacteriol 1998;180:6269–6275. [PubMed: 9829936]
58. Talpaert-Borle M, Campagnari F, Creissen DM. Properties of purified uracil-DNA glycosylase from calf thymus. An in vitro study using synthetic DNA-like substrates. J Biol Chem 1982;257:1208–1214. [PubMed: 7056715]
59. Domena JD, Timmer RT, Dicharry SA, Mosbaugh DW. Purification and properties of mitochondrial uracil-DNA glycosylase from rat liver. Biochemistry 1988;27:6742–6751. [PubMed: 3196681]
60. Huang JM, Anastos AK, Robison E, Shi R, Freeman K, Strickler H, Steinberg JJ. Evaluation of DNA adduction of AZT in peripheral blood leukocytes of HIV-infected individuals by (32)P-post-labeling thin-layer chromatography: a feasibility study. J Chromatogr B 2004;810:1–6.
61. Summers WC, Raksin P. A method for selection of mutations at the tdk locus in *Escherichia coli*. J Bacteriol 1993;175:6049–6051. [PubMed: 8376351]
62. Jensen KF, Leer JC, Nygaard NP. Thymine utilization in *Escherichia coli* K12 on the role of deoxyribose 1-phosphate and thymidine phosphorylase. Eur J Biochem 1973;40:345–354. [PubMed: 4592648]
63. Barabas O, Pongracz V, Kovari J, Wilmanns M, Vertessy BG. Structural insights into the catalytic mechanism of phosphate ester hydrolysis by dUTPase. J Biol Chem 2004;279:42907–42915. [PubMed: 15208312]
64. Fiser A, Vertessy BG. Altered subunit communication in subfamilies of trimeric dUTPases. Biochem Biophys Res Commun 2000;279:534–542. [PubMed: 11118321]
65. Kubareva EA, Vasilenko NL, Vorobjeva OV, Volkov EM, Oretskaya TS, Korshunova GA, Nevinsky GA. Role of DNA definite structural elements in interaction with repair enzyme uracil-DNA glycosylase. Biochem Mol Biol Int 1998;46:597–606. [PubMed: 9818099]
66. Neuhard, J. Utilzation of Preformed Pyrimidine Bases and Nucleosides. Academic Press; New York: 1983.
67. Crott JW, Mashiyama ST, Ames BN, Fenech MF. Methylenetetrahydrofolate reductase C677T polymorphism does not alter folic acid deficiency-induced uracil incorporation into primary human lymphocyte DNA in vitro. Carcinogenesis 2001;22:1019–1025. [PubMed: 11408344]

NIH-PA Author Manuscript

NIH-PA Author Manuscript

NIH-PA Author Manuscript

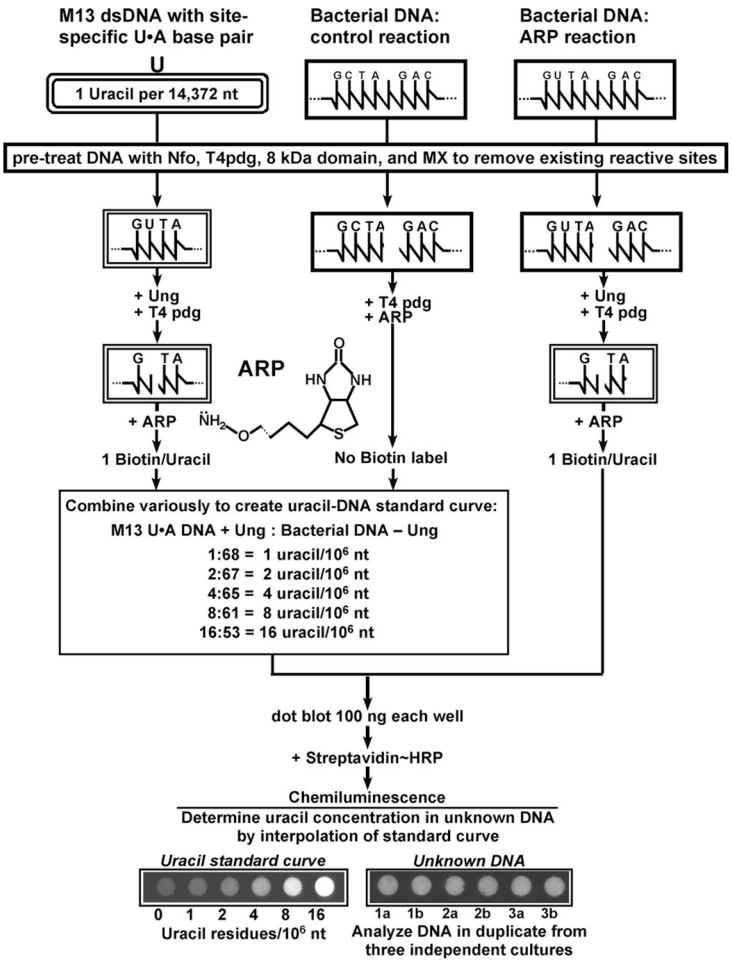

Fig. 1.
Scheme for quantitative detection of uracil residues in DNA.

NIH-PA Author Manuscript

NIH-PA Author Manuscript

NIH-PA Author Manuscript

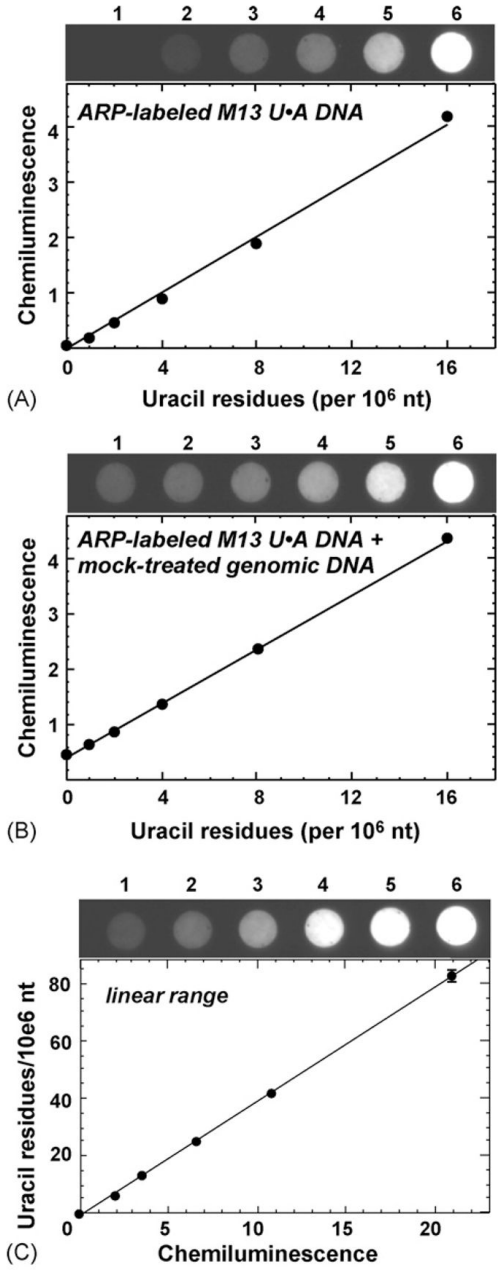

Fig. 2.

Standard curve for measuring uracil-DNA. (A) Chemiluminescence (arbitrary units) of M13 U·A DNA samples containing 0, 1, 2, 4, 8, or 16 U/10^6 nt (lanes 1–6, respectively). Samples without control genomic DNA were prepared in duplicate (only one set of samples is shown) as described under Section 2. Error bars representing the standard deviation are hidden by plot symbols. (B) Chemiluminescence of M13 U·A DNA combined with control genomic DNA. Samples were prepared in duplicate; error bars are hidden by plot symbols. (C) Linear range of the Ung-ARP assay. Chemiluminescence intensity was recorded as a function of increasing amounts (U/10^6 nt) of uracil-rich DNA from *Escherichia coli* CJ236.

NIH-PA Author Manuscript

NIH-PA Author Manuscript

NIH-PA Author Manuscript

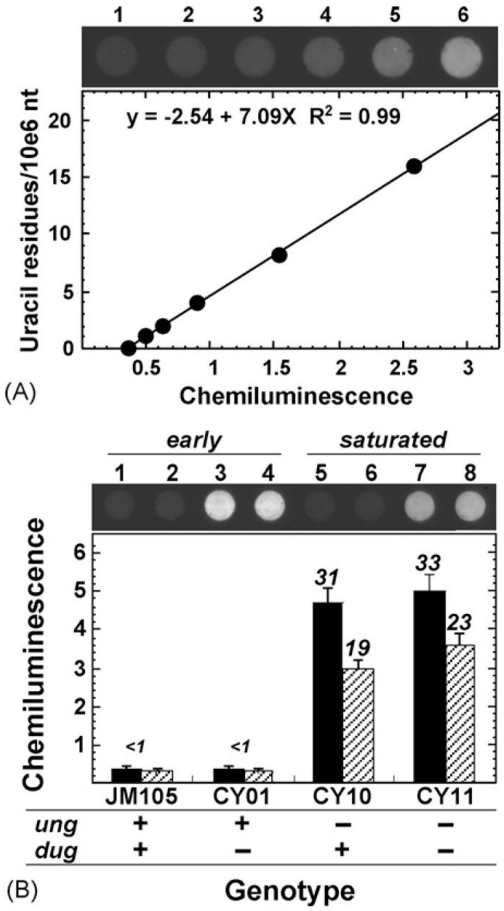

Fig. 3.

Uracil accumulation in isogenic *E. coli ung dug* mutants. (A) Standard curve of Ung-ARP-associated chemiluminescence constructed using JM105 (*ung*$^+$ *dug*$^+$) control DNA and M13 U·A DNA as shown in Fig. 2B. A digital image of the dot blot chemiluminescence is shown. Lanes 1–6 correspond to samples containing 0, 1, 2, 4, 8, and 16 U/10^6 nt, respectively. A graph of the chemiluminescence intensity of the samples is shown below the image. An equation (inset) relates the uracil-DNA concentration (U/10^6 nt) of the standards as a function of chemiluminescence intensity; R^2 represents the coefficient of determination. The negative intercept indicates a background chemiluminescence of 0.36 arbitrary units from JM105 DNA. (B) Uracil accumulation in *ung dug* mutants of JM105. Mutant strains were constructed as described under Section 2 and grown in minimal medium supplemented with Norit-treated casamino acids. Genomic DNA from early (solid bars) and late (striped bars) log phase growth cultures was analyzed for uracil accumulation using the standard curve shown in (A). A digital image of the dot blot chemiluminescence is shown. Samples in lanes 1–4 were respectively purified from JM105, CY01, CY10, and CY11 cultures in early log phase growth; samples in lanes 5–8 were from the respective JM105, CY01, CY10, and CY11 cultures in late log phase growth. Numbers over the bars indicate the amount of uracil residues per million nucleotides. Errors represent the standard deviation of three independent determinations.

NIH-PA Author Manuscript

NIH-PA Author Manuscript

NIH-PA Author Manuscript

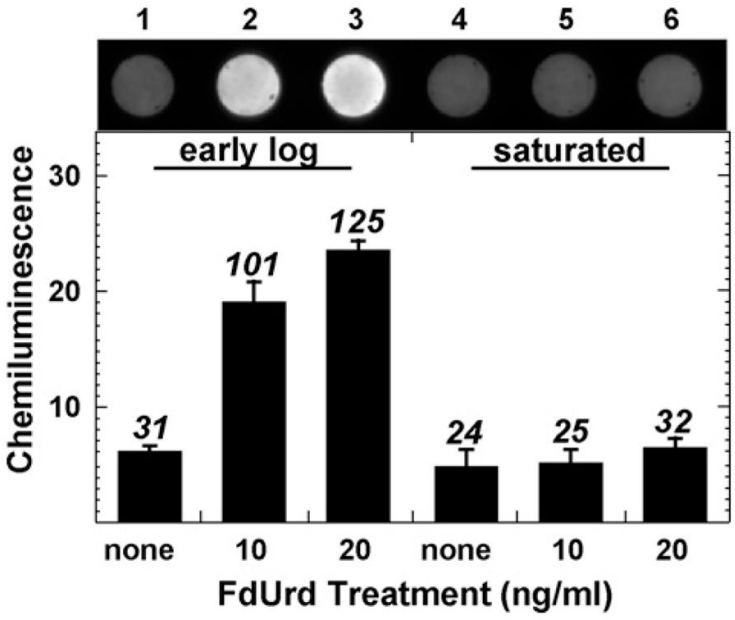

Fig. 4.

Effect of 5-fluoro-2′-deoxyuridine on uracil accumulation in CY11 genomic DNA. Cultures of CY11 (*ung dug*) were propagated in the presence of 0, 10, and 20 ng/ml of 5-fluoro-2′-deoxyuridine, harvested at either early log or saturated growth phase as indicated, and the DNA was extracted and subjected to the Ung-ARP assay. An image of the chemiluminescence reaction is shown about the bar graph. The level of uracil residues was determined by means of the uracil-DNA standard curve (image not shown). Numbers above the bars indicate the number of uracil residues per million nucleotides.

NIH-PA Author Manuscript
NIH-PA Author Manuscript
NIH-PA Author Manuscript

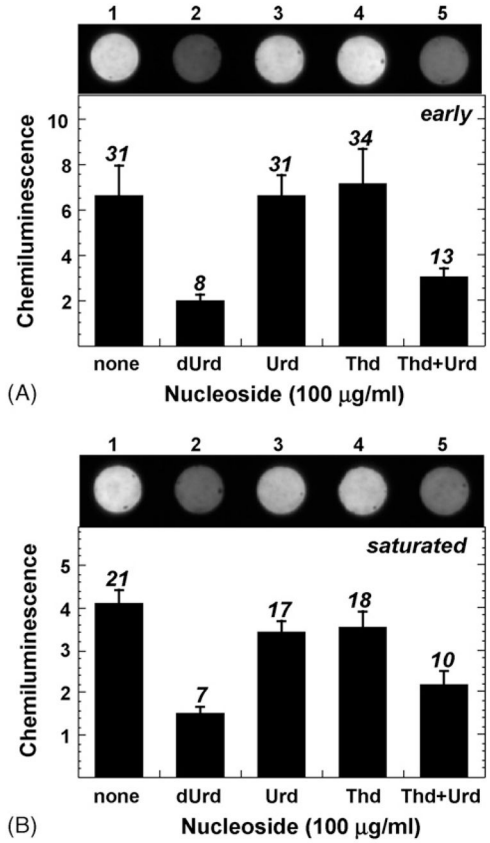

Fig. 5.

Effect of nucleoside supplementation on uracil accumulation in CY11 (*ung dug*) DNA. (A) Early log phase growth; (B) saturated phase growth. DNA from CJ236 cultures supplemented (100 μg/ml) as indicated with either dUrd, Urd, Thd, Thd and Urd, or not at all, was subjected to the Ung-ARP assay. An image of each chemiluminescence reaction is shown about the bar graph. The level of uracil residues was determined by means of a uracil-DNA standard curve (not shown). Numbers above the bars indicate the number of uracil residues per million nucleotides.

NIH-PA Author Manuscript

NIH-PA Author Manuscript

NIH-PA Author Manuscript

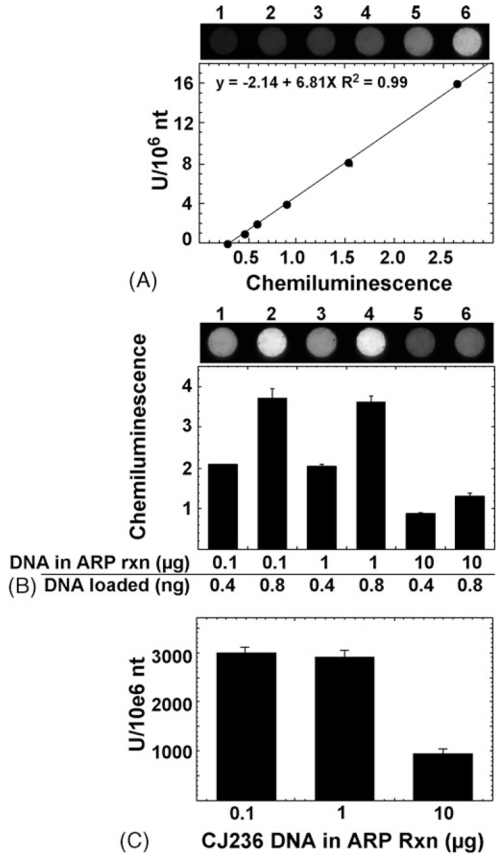

Fig. 6.

Determination of uracil residues in CJ236 (*dut-1 ung-1*) genomic DNA. (A) Uracil-DNA standard curve, constructed as described under Fig. 3. Lanes 1–6 correspond respectively to samples containing 0, 1, 2, 4, 8, and 16 U/10^6 nt. (B) Chemiluminescence of early log CJ236 DNA. The amount of CJ236 in the Ung-ARP reaction as well as the amount of ARP-labeled DNA applied to the dot blot is listed below each column of the bar graph and corresponds to lanes 1–6 of the chemiluminescence digital image. JM105 control DNA was added to bring the total amount of DNA applied to the dot blot to100 ng. Error bars represent the standard deviation of the chemiluminescence intensity of two determinations. (C) The level of uracil in early log CJ236 DNA was calculated based on the standard curve shown in (A) and the average chemiluminescence intensity of each reaction condition shown in (B).

NIH-PA Author Manuscript
NIH-PA Author Manuscript
NIH-PA Author Manuscript

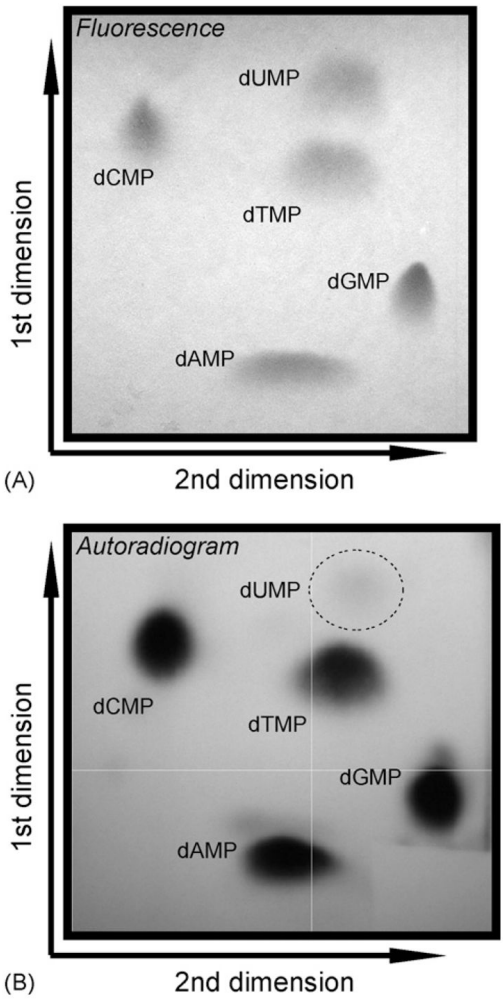

Fig. 7.

Two-dimensional thin-layer chromatography of CJ236 32P 2′-deoxynucleoside 5′-monophosphates. (A) Fluorescence image of CJ236 2′-deoxynucleoside 5′-monophosphates on a PEI-cellulose sheet subjected to two-dimensional thin-layer chromatography. CJ236 DNA (20 μg) was digested to 5′-dNMPs, filtered, supplemented with 5′-dUMP, and applied to a PEI-cellulose sheet as described under Section 2. (B) ^{32}P autoradiogram of the PEI-cellulose sheet shown in (A).

NIH-PA Author Manuscript

NIH-PA Author Manuscript

NIH-PA Author Manuscript

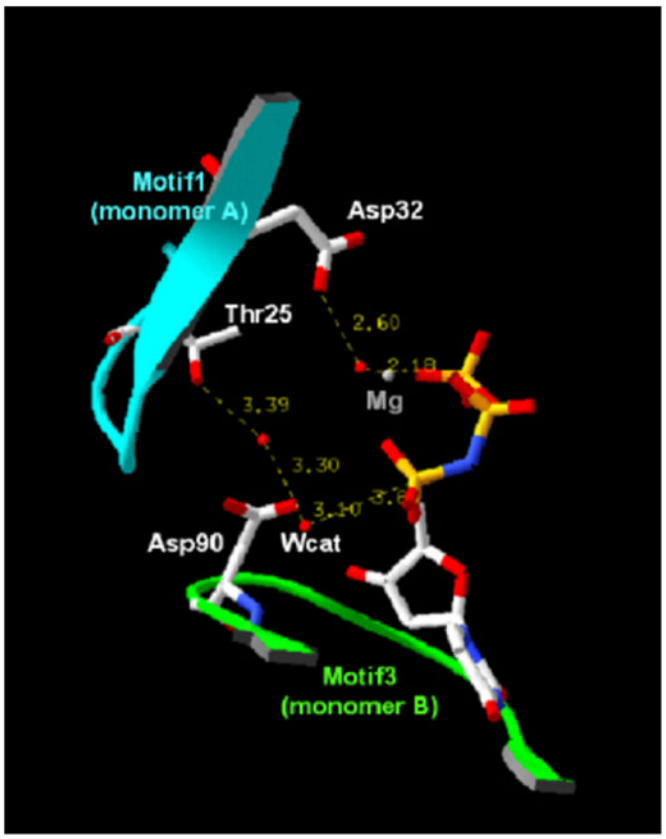

Fig. 8.

Coordination environment of Thr24 in *E. coli* dUTP pyrophosphatase. A part of the active site is shown from the crystal structure of *E. coli* dUTP pyrophosphatase in complex with an α,β-imino-dUTP substrate analogue (adapted from Barabas et al. [63]. The backbone of Motif 1 from monomer A is cyan, and that of Motif 3 from monomer B is green. Side chain and ligand (Mg^{2+} and α,β-imino-dUTP) are in atomic coloring (O, red, N, blue, P, yellow, C, white). H-bonds are dashed yellow, lengths are given in angstroms. Wcat indicates the catalytic water molecule in-line with the scissile bond. Two other waters are shown: one is coordinated both to Asp90 and Thr25, while the other is within the Mg-sphere (shown for orientation reasons only). Numbering is according to the PDB file reported in Barabas et al. [63] where the protein possessed an additional Met at the N-terminus because of cloning; therefore, Thr25 is Thr24 in the original sequence. (For interpretation of the references to colour in this figure legend, the reader is referred to the web version of the article.)

NIH-PA Author Manuscript

NIH-PA Author Manuscript

NIH-PA Author Manuscript

Table 1

Incorporation of $^{32}P_i$ into CJ236 DNA at 30 °C

2′-Deoxynucleoside 5′-monophosphate	% ^{32}P radioactivity	U/10^6 nt[a]	U/(U + T) ratio[b] (U/10^6 nt)[c]
dCMP	24.8 ± 0.02[d]		
damp	21.4 ± 0.02		
dGMP	35.9 ± 0.04		
dTMP	17.2 ± 0.03		
dUMP	0.66 ± 0.12	6644 ± 1179	0.0372 ± 0.0029 (9300 ± 725)[c]

[a] Determined by dividing dUMP ^{32}P cpm by total ^{32}P cpm detected and multiplying by 10^6.

[b] Quotient of dUMP ^{32}P cpm divided by the sum of dUMP and dTMP ^{32}P cpm.

[c] Determined by multiplying the ratio, defined in Footnote b, by 250,000, the average number of dTMP residues in 10^6 nt.

[d] ± Represents the standard deviation of four independent measurements.

NIH-PA Author Manuscript

NIH-PA Author Manuscript

NIH-PA Author Manuscript

Table 2

Incorporation of ^{3}H from [6-^{3}H]Uracil into CJ236 DNA at 30 °C

2′-Deoxynucleoside 5′-monophosphate	% ^{3}H radioactivity	U/(U + T) ratio[a] (U/10^{6} nt)[b]
dCMP	64.7	
damp	0.75	
dGMP	0.33	
dTMP	31.6	
dump	2.58	0.0754 (18,850)

[a] Quotient of dUMP ^{3}H cpm divided by the sum of dUMP and dTMP ^{3}H cpm.

[b] Determined by multiplying the ratio, defined in Footnote a, by 250,000 (see Footnote c of Table 1).

NIH-PA Author Manuscript

NIH-PA Author Manuscript

NIH-PA Author Manuscript

Table 3

LC/MS analysis of deoxyuridine:thymidine ratios in CJ236 DNA

2′-Deoxynucleoside	Deoxynucleoside/base[a]	(dUrd/U) to (dThd/T) ratio (U/10^6 nt)[b]
dUrd	15033 ± 611[c]	
dThd	476670 ± 72858	0.0320 ± 0.004 (7752)

[a] Arbitrary intensity units.

[b] Calculated by multiplying the (dUrd/U):(dThd/T) ratio by 250,000 and dividing by 1.032.

[c] ± Represents the standard deviation of three measurements.